Frontiers in Heat and Mass Transfer (FHMT), 19, 7 (2022)
DOI: 10.5098/hmt.19.7

Global Digital Central
ISSN: 2151-8629

Frontiers in Heat and Mass Transfer

Available at www.ThermalFluidsCentral.org

ANALYTICAL STUDY OF THERMAL PERFORMANCE OF A JET PLATE SOLAR AIR HEATER WITH THE LONGITUDINAL FINS UNDER THE CROSS FLOW AND NON-CROSS FLOW CONDITIONS

Rajen Kumar Nayak[a,*], Ravi Shankar Prasad[a,†], Ujjwal Kumar Nayak[a], Amit Kumar Gupta[b]

[a] *Department of Mechanical Engineering, B.I.T. Sindri, P.O.: Sindri Institute, Sindri, Dhanbad, Jharkhand PIN 828123 India*
[b] *Department of Chemical Engineering, B.I.T. Sindri, P.O.: Sindri Institute, Sindri, Dhanbad, Jharkhand PIN 828123 India*

ABSTRACT

This analytical study has been carried out on inline and staggered hole jet plate solar air heater with longitudinal fins attached underside the absorber surface under the cross flow and non-cross flow conditions of air through the channels for varying mass flow rate of air, $\dot{m}_1$ (50-300 kg/hm^2), jet hole diameter, D (6 mm-10 mm) and distance between the absorber and jet plate, Z_2 (5 cm-10 cm) with fixed number of jet holes, N (480 and 1008 for inline and staggered hole respectively) and pitch of the fins, p (3 mm). The result shows the performance of staggered hole jet plate solar air heater with longitudinal fins under non-cross flow is better than cross flow condition. The increment of T_o and h_{Pj} are found higher in non-cross flow staggered hole jet plate solar air heater with longitudinal fins at smaller jet hole diameter, D (6 mm) than larger jet hole diameter, D (8 mm and 10 mm) for fixed $\dot{m}_1$ (50 kg/hm^2). For fixed mass flow rate of air, $\dot{m}_1$ (50-300 kg/hm^2), the outlet air temperature (T_o) and collector efficiency (η_c) are obtained higher at lower Z_2 (5 cm) with respect to larger Z_2 (6 cm-10 cm). For the fixed Reynolds number (Re_{ja2}), the required pumping power may be less or high in non-cross flow staggered hole jet plate than non-cross flow inline hole jet plate air heater with longitudinal fins attached underside the absorber surface.

Keywords: c*ross flow, non-cross flow, inline hole, staggered hole, jet plate, fins, solar energy.*

1. INTRODUCTION

Presently, the utilization of renewable and non-conventional sources of energy is one of the most discussed, contemporary and prevalent issues around the world. In many parts of the world, the shortage of fossil fuel has become a matter of serious concern and the prices of fossil fuels have been increased sharply and it is clear indication that the reserves of fossil fuel or nonrenewable resources of energy (oil, coal and natural gas) is gradually coming to the end. So, this realization has triggered the urgent need for alternative sources of energy.

Out of many alternative energy sources, solar energy is one of the most promising options to make extensive use of renewable sources of energy, which is derived from the sun. The power from the sun intercepted by earth is approximately 1.8 x 10^{11} MW, which is many thousand times larger than present consumption rate on the earth from all the commercial sources of energy. The potential availability of this energy is about 20 MW/sq. km, but presently only 1.74 MW/sq. km is potentially exploited through present technology (Sukhatme, S.P., 1996).

Solar energy is used for water heating, cooking and crops drying etc. The most important component of solar energy utilization systems are solar collectors. Conventionally, flat plate solar air heaters are used for space heating and drying of agricultural products. However, non-conventional jet plate solar air heater is being used extensively for space heating and agricultural products drying due to its high convective heat transfer coefficient and collector efficiency.

Perry (1954) studied the convective heat transfer from a hot gas jet to a plane surface and suggested that the heat transfer coefficient is higher in non-conventional jet impingement solar air heater than the conventional solar air heater. Gupta and Garg (1967) presented an extensive performance study on solar air heaters. Kercher and Tabakoff (1970) studied the heat transfer by a square array of round air jets impinging perpendicular to a flat surface including the effect of spent air and presented the heat transfer correlation, which is most applicable for the configuration of jet concept solar air heater. Metzger *et al.* (1979) studied the heat transfer characteristics for inline and staggered arrays of circular jets with cross flow of spent air. Heat transfer characteristics were measured for the two-dimensional arrays of jets impinging on a surface parallel to the jet orifice plate. Florschuetz *et al.* (1981) have observed the behaviour of heat transfer coefficient in inline and staggered hole jet plate for various pitch of the jet holes. Garg *et al.* (1983) performed a study on the effect of enhanced heat transfer area in solar air heaters. Prasad and Saini (1988) analyzed the effect of artificial roughness on friction factor and enhancing heat transfer in a solar air heater. Garg et al. (1989) presented the performance studies on a finned solar air heater. Garg *et al.* (1990) made a theoretical analysis on a new finned type solar air heater.

Chaudhury and Garg (1991) evaluated the temperature increment and performance efficiency of jet concept air heater over that of flat plate solar air heater. With a duct depth of 10 cm and length of 2.0 m, the rise in temperature is 15.5°C to 2.5°C and rise in efficiency is around 26.5% to 19.0%, respectively, for air flow rate in the range 50 to 250 kg/hm^2. Garg *et al.* (1991) performed a theoretical analysis on a new finned type solar air heater. Verma et al. (1991) performed parametric studies on the corrugated solar air heaters with and without cover. Gupta *et al.* (1993) studied heat and fluid flow in rectangular solar air heater ducts having

* Department of Mechanical Engineering, B.I.T. Sindri, P.O.: Sindri Institute, Sindri, Dhanbad, Jharkhand PIN 828123 India
† *Corresponding author. Email: rsprasad.me@bitsindri.ac.in*

Global Digital Central
ISSN: 2151-8629

transverse rib roughness on absorber plates. This experimental investigation was carried out in the solar air heater ducts with absorber plates having transverse wire roughness in transitionally rough flow region. Thombre and Sukhatme (1995) studied turbulent flow heat transfer and friction factor characteristics of shrouded fin arrays with uninterrupted fins and developed the correlation for determining the values of the convective heat transfer coefficient and the pressure drop on finned solar air heater experimentally.

Sahu and Bhagoria (2005) made augmentation of heat transfer coefficient by using 90° broken transverse ribs on absorber plate of solar air heater. Irfan and Emre (2006) performed an experimental investigation of solar air heater with free and fixed fins and estimated the efficiency and exergy loss. Jourker *et al.* (2006) studied the heat transfer and friction characteristics of solar air heater duct using rib grooved artificial roughness. The conditions for best performance were found and correlations for Nusselt number and friction factor was presented. Kurtbas and Turgut (2006) made an experimental investigation of efficiency, energy loss and performance of solar air heater with free and fixed fins and compared the heat transfer coefficient and output air temperature. Singh (2006) analyzed heat transfer enhancement in a continuous longitudinal fin solar air heater at different pitches. Karsli (2007) made a performance analysis of new design solar air collectors for drying applications. Romdhane (2007) made a comparative study of the air solar collectors and studied the heat transfer with the introduction of baffles to favor the heat transfer. Belusko *et al.* (2008) discussed the improvement of thermal efficiency of an unglazed solar air heater by using the jet impingement. Aharwal *et al.* (2009) studied the heat transfer and friction characteristics of solar air heater ducts having integral inclined discrete ribs on absorber plate. The use of artificial roughness in a solar air heater duct was proposed to enhance the heat transfer from the absorber plate to the air. An experimental investigation on heat transfer and friction characteristics of solar air heater ducts with integral repeated discrete square ribs on the absorber plate was presented. The effects of geometrical parameters like the gap width and gap position were studied. Akpinar and Kocyigit (2010) made an experimental investigation of thermal performance of solar air heater having different obstacles on absorber plates. Xing *et al.* (2010) performed an experimental and numerical investigation of heat transfer characteristics of inline and staggered arrays of impinging jets. The heat transfer coefficient was calculated by measuring the local jet temperatures at several positions on the impingement plate.

Chabane *et al.* (2013a) analyzed the collector efficiency by single pass of solar air heaters with and without using fins. Chabane *et al.* (2013b) performed a thermal efficiency analysis of a single flow solar air heater with different mass flow rates in a smooth plate. Chauhan and Thakur (2013) carried out an experimental investigation on heat transfer and friction factor characteristics by using impinging jet solar air heater. Chabane *et al.* (2014) made an experimental study of heat transfer and thermal performance with longitudinal fins of solar air heater. Nayak and Singh (2016) studied the effect of geometrical aspects on the performance of jet plate solar air heater. Aboghrara *et al.* (2017) made a performance analysis of solar air heater with jet impingement on corrugated absorber plate. Hasan *et al.* (2017) made an experimental investigation of jet array nano-fluids impingement in photovoltaic thermal collector. Nadda *et al.* (2017) analyzed the heat transfer and friction loss in an impingement jets solar air heater with multiple arc protrusion obstacles. Rajaseenivasan *et al.* (2017) made an experimental investigation on the performance of an impinging jet solar air heater. Soni and Singh (2017) made an experimental analysis of geometrical parameters on the performance of an inline jet plate solar air heater. Vinod and Singh (2017) analyzed the thermo-hydraulic performance of jet plate solar air heater under cross flow condition. Aboghrara *et al.* (2018) performed a parametric study on the thermal performance and optimal design elements of solar air heater enhanced with jet impingement on a corrugated absorber plate. Matheswaran *et al.* (2018) performed an analytical investigation of solar air heater with jet impingement using energy and exergy analysis. Sivakumar *et al.* (2019) performed an experimental thermodynamic analysis of a forced convection solar air heater using absorber plate with pin fins. Kumar *et al.* (2020) developed the new correlations for heat transfer and pressure loss due to internal conical ring obstacles in an impinging jet solar air heater passage. Singh *et al.* (2020) utilized the circular jet impingement to enhance thermal performance of solar air heater. Yadav and Saini (2020) made a numerical investigation on the performance of a solar air heater using jet impingement with absorber plate.

Farahani and Shadi (2021) suggested an optimization-decision making of roughened solar air heaters with impingement jets based on efficiency of energy and exergy as well as costs analysis. Hassan and AboElfadl (2021) made a heat transfer and performance analysis of solar air heater having new transverse finned absorber of lateral gaps and central holes. Kumar *et al.* (2021a) studied the heat transfer and developed the friction factor correlations for an impinging air jets solar thermal collector with arc ribs on an absorber plate. Kumar *et al.* (2021b) made a comprehensive review of performance analysis of with and without fins solar thermal collector. Maithani *et al.* (2021) made a thermo-hydraulic and exergy analysis of inclined impinging jets on absorber plate of solar air heater. Moshery *et al.* (2021) studied the thermal performance of jet-impingement solar air heater with transverse ribs absorber plate. Pazarlioğlu *et al.* (2021) made a numerical analysis of the effect of impinging jet on cooling of solar air heater with longitudinal fins. Salman *et al.* (2021a) made an exergy analysis of solar heat collector with air jet impingement on dimple shaped roughened absorber surface. Salman *et al.* (2021b) performed an experimental analysis of single loop solar heat collector with jet impingement over indented dimples. Shetty *et al.* (2021) made a numerical analysis of a solar air heater with circular perforated absorber plate.

Das *et al.* (2022) made a numerical analysis of a solar air heater with jet impingement and compared between the performance of different jet designs. Flilihi *et al.* (2022) studied the effect of absorber design on convective heat transfer in a flat plate solar collector through a CFD modeling. Salman *et al.* (2022) studied the utilization of jet impingement on dimple shaped protrusion on heated plate to improve the performance of double pass solar heat collector. Yadav and Saini (2022) made a thermo-hydraulic CFD analysis of impinging jet solar air heater with different jet geometries.

The several researchers including Chaudhury and Garg (1991), Singh (2006), Kercher and Tabakoff (1970) studied the heat transfer characteristics for impinging jet air solar heaters of single and two-dimensional array of circular air jets.

However, the critical search of the literatures shows there only a very few literatures are available about the jet plate solar air heater. There a very few analytical research papers are available on the performance of nonconventional jet plate solar air heater with longitudinal fins so far. So, the present analytical work is aimed to investigate experimentally the performance of inline and staggered hole jet plate solar air heater with longitudinal fins attached underside of the absorber surface under cross and non-cross flow conditions.

2. THEORETICAL ANALYSIS

Fig.1 shows the schematic diagram of the jet plate solar air heater, which consists of blower, bottom plate, jet plate with inline and staggered hole (shown in Figs. 2 and 3 respectively), black painted absorber plate with attached fins underside the absorber surface ($\alpha = 0.95$), toughened glass cover plate ($\tau = 0.90$), jet plate inserted between absorber and bottom plate, two flow channels, bottom and side insulation ($k_i = 0.034$ W/mK) of thickness 5 cm and thermocouples imbedded to each plate. In case of cross flow condition, mass flow rate of air ($\dot{m}_1$) between bottom plate and jet plate impinges out of the jet holes on the jet plate and mixes with $\dot{m}_2$ in the upper channel as shown in Fig. 4 and subsequently the same comes out from the upper channel exit. Similarly, for non-cross flow condition, since inlet of upper channel is closed so air ($\dot{m}_1$) from the bottom channel

Global Digital Central
ISSN: 2151-8629

passes through the jet holes and strikes the lower surface of the absorber plate, finally air ($\dot{m}_1$) comes out from the upper channel exit as shown in Fig. 5. The sectional view of the absorber plate with and without fins attached to the absorber plate is shown in Fig. 6. The supply air $\dot{m}_1$ and $\dot{m}_2$ may be regulated or controlled with the help of a voltage regulator, which is integrated with the air blower. Similarly, the absorber plate temperature (T_P), jet plate temperature (Tj) and bottom plate temperature (T_b) can be measured with the help of thermocouples which are embedded on the plates separately, whereas the ambient temperature (T_A) and wind velocity (V_w) can be recorded with the help of hot wire anemometer. The solar intensity is recorded with the help of a pyranometer. The whole structure is supported on a movable steel frame. The specification of the setup is tabulated in the Table. 1.

Table 1 Specifications of the set up

Nomenclature	*Specification*
Length of collector	L = 2.0 m
Width of collector	W = 1.0 m
Total channel depth	Z = 14 cm
Depth of lower channel	Z_1 = 7 cm, 8 cm
Depth of upper channel	Z_2 = 6 cm, 7 cm
Diameter of jet holes	D = 6 mm, 8 mm and 10 mm
Hydraulic diameter for flat – plate solar air heater	D_h = 0.246m
Hydraulic diameter of the upper channel in jet plate air heater	D_2 = 0.12m (for Z_2 = 6 cm) D_2 = 0.13m (for Z_2 = 7 cm)
Hydraulic diameter of the upper channel in jet plate with longitudinal fins air heater	D_e = 0.12m
Number of inline holes	N = 561
Number of staggered holes	N = 1173
Stream-wise pitch	X = 43 mm
Span-wise pitch	Y = 6 cm
Absorber plate	t = 1 mm
Jet plate	t = 4 mm,
Glass cover	t = 4 mm
Air thickness	d = 2.54 cm
Length of fins	L = 2 m
Height of fins	L_f = 12 mm
Thickness of fins,	δ_f = 3 mm
Number of fins	N_f = 20
Tilt angle	θ = 22.6°
Base and side insulation	t = 25 mm
Thermal conductivity of the fins	k_{Al} = 237 W/mK

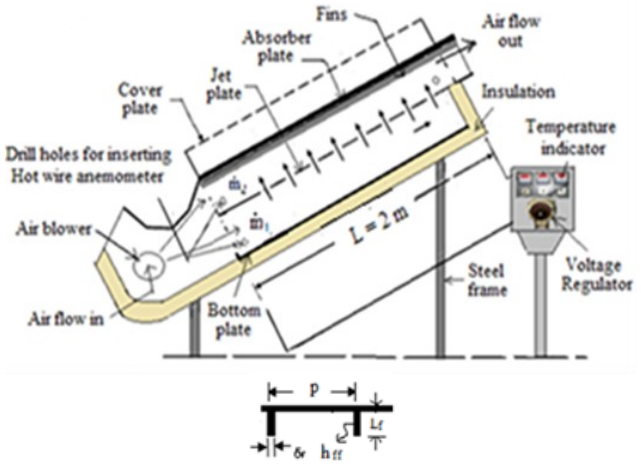

Fig. 1 Schematic diagram of the jet plate solar air heater with longitudinal fins attached underside the absorber surface along with elemental section of the absorber plate

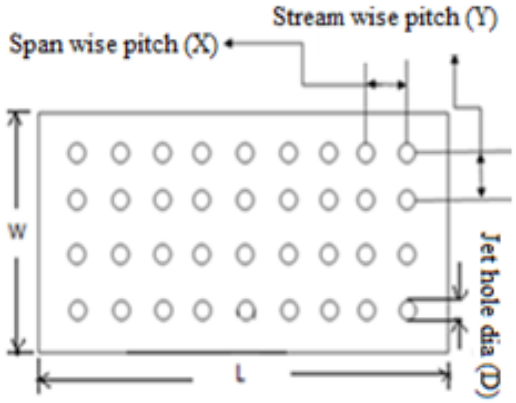

Fig. 2 Jet plate with inline holes

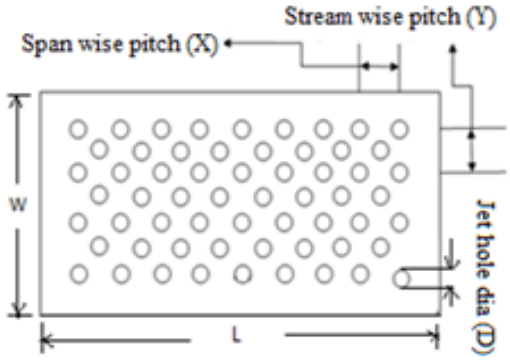

Fig. 3 Jet Plate with staggered holes

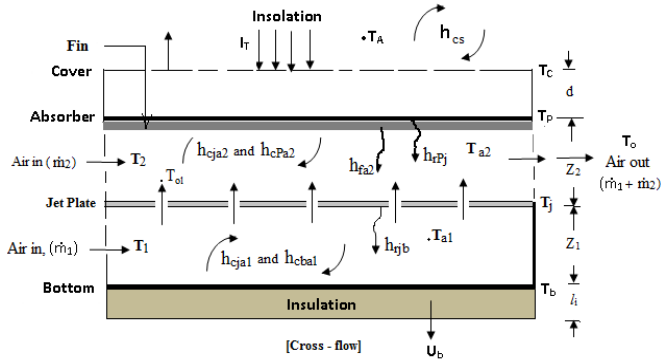

Fig. 4 Sectional view of cross flow jet plate solar air heater with longitudinal fins underside the absorber surface

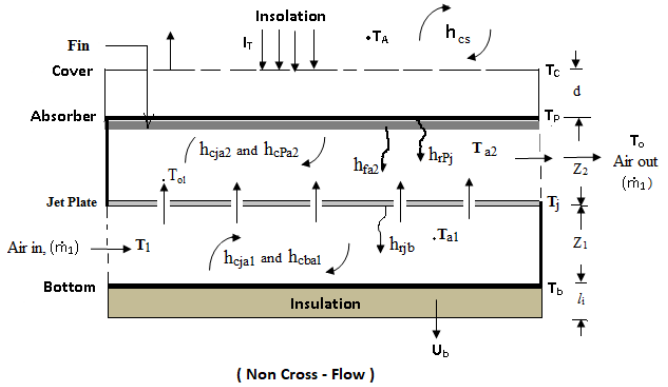

Fig. 5 Sectional view of non-cross flow jet plate solar air heater with longitudinal fins underside the absorber surface

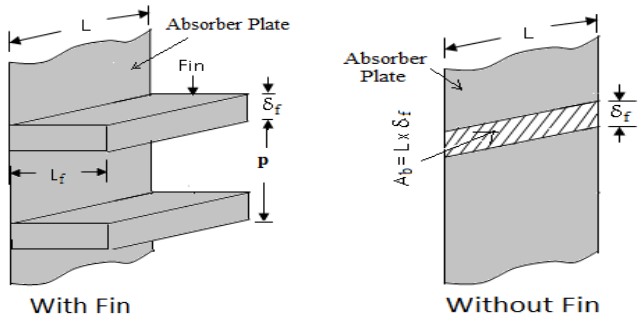

Fig. 6(a) With fins **Fig. 6(b)** Without fins
Fig. 6 Sectional view of absorber plate with and without fins

2.1 Energy balance equation for jet plate solar air heater with longitudinal fins attached underside the absorber surface under steady state condition (Chaudhury and Garg, 1991)

For computing the performance of jet plate with longitudinal fins attached underside the absorber surface, the following equations are used under steady state condition.

For the cover plate,

$$h_{CS}(T_C - T_A) = h_{PC}(T_P - T_C) \quad (1)$$

For absorber plate,

$$I\tau\alpha = h_{PC}(T_P - T_C) + h_{cPa2}(T_P - T_{a2}) + h_{rPj}(T_P - T_j) + 2L_f \xi h_{fa2}(T_P - T_{a2}) / p \quad (2)$$

For jet plate,

$$h_{rPj}(T_P - T_j) = h_{cja2}(T_j - T_{a2}) + h_{cja1}(T_j - T_{a1}) + h_{rjb}(T_j - T_b) \quad (3)$$

For bottom plate,

$$h_{rjb}(T_j - T_b) = h_{cba1}(T_b - T_{a1}) + U_b(T_b - T_A) \quad (4)$$

For air stream between jet plate and bottom plate,

$$\dot{m}_1 C(T_{ol} - T_A) = h_{cja1}(T_j - T_{a1}) + h_{cba1}(T_b - T_{a1}) \quad (5)$$

The rate of useful heat gain (Q_u) in air stream between absorber plate and jet plate be,

$$Q_u = \dot{m}_1 C_p(T_o - T_{ol}) + \dot{m}_2 C_p(T_o - T_A) = h_{cja2}(T_j - T_{a2}) + h_{cPa2}(T_P - T_{a2}) + 2L_f \xi h_{fa2}(T_P - T_{a2}) / p \quad (6)$$

Similar, to jet plate air heater in equations (1) to (6),

$T_{a1} = (T_A + T_{ol}) / 2$

$T_{a2} = (T_i + T_o) / 2$

and $T_i = (\dot{m}_1 T_{ol} + \dot{m}_2 T_A) / (\dot{m}_1 + \dot{m}_2)$

Hence, the collector efficiency (η_c) be,

$$\eta_c = (\dot{m}_1 + \dot{m}_2) C_p(T_o - T_A) / I_T A \quad (7)$$

where, $\dot{m}_1 = \rho(WZ_1)\bar{v}_1$ and $\dot{m}_2 = \rho(WZ_2)\bar{v}_2$

Now, the convective heat transfer coefficient between absorber plate-to-air stream in the upper channel can be computed from,

$$h_{Pj} = (\dot{m}_1 + \dot{m}_2) C_p(T_o - T_i) / A(T_P - T_{a2}) \quad (8)$$

Similarly, the Nusselt number ((Nu_{Pj}) and Reynolds number (Re_{ja2}) in the upper channel can be calculated from,

$$Nu_{Pj} = h_{Pj} D_e / k_a = F_1 F_2 (Re_D)^m (Z_2/D)^{0.091} \quad (9)$$

$$Re_{ja2} = \rho\bar{v} D_e / \mu \quad (10)$$

where, $\bar{v} = (V_{av} + \bar{v}_o) / 2$, $V_{av} = (A_j V_j + A_2\bar{v}_2) / (A_2 + A_j)$,

$Re_D = \rho V_j D/\mu$, $V_j = 4\dot{m}_1 / N\rho\pi D^2$ and $D_e = 4[pZ_2 - L_f \delta_f] / 2[(p + L_f]$ (Sukhatme, 1996)

The friction factor (f_s) can be calculated from the Blasius equation as,

$$f_s = 0.085(\rho \bar{v} D_2/\mu)^{-0.25} = 0.085(Re_{ja2})^{-0.25} \quad (11)$$

Since, the fins are attached underside the absorber surface. So, it is need to find the performance of the fins. The fin efficiency (η_f) and fin effectiveness (ξ) of the rectangular fin are defined as,

η_f = [(Actual heat transfer rate from the fins) / (Ideal heat transfer rate from the fin if the entire fins are at base temperature)]

or, $\eta_f = (Q_f / Q_{mf}) = (h_{Pj} P_f k_{Al} A_c)^{1/2} (T_P - T_{a2}) / h_{Pj} A_f (T_P - T_{a2})$

$$\text{or, } \eta_f = \tanh(m' L_c) / (m L_c) \quad (12)$$

where, $m' L_c = L_c [(2 h_{Pj}) / (k_{Al} \delta_f)]^{1/2}$,

L_c (Corrected length) $= L_f + \delta_f / 2$

and $m' = [(h_{Pj} P_f / (k_{Al} A_c)]^{1/2}$

2.2 The Fin Effectiveness

The effectiveness of the fin, $\xi = (Q_f / Q_{Nf})$

or, $\xi = (h_{Pj} P_f k_{Al} A_c)^{1/2} (T_P - T_{a2}) / h_{Pj} A_b (T_P - T_{a2})$

$$\text{or, } \xi = [(k_{Al} P_f) / (h_{Pj} A_b)]^{1/2} \quad (13)$$

where, $P_f = (2L_f + \delta_f)$ and $A_b = L \times \delta_f$

The value of $\dot{m}_2$ is zero (i.e., $\dot{m}_2 = 0$) for non-cross flow condition.

In the present work, the collector efficiency (η_c), instantaneous efficiency (η_i), heat transfer coefficient (h_{Pj}), Reynolds number (Re_{ja2}), friction factor (f_s) and fin efficiency are determined from the above equations (1) to (12) respectively, for cross flow and non-cross flow jet plate with longitudinal fins solar air heater whereas the fin effectiveness is calculated from equation (13).

2.3 Heat Transfer Coefficients (Chaudhury and Garg, 1991)

The convective heat transfer coefficient, h_w, for air flowing over the outer surface of the glass cover depends on wind velocity V_w (McAdams, 1954). Thus, the obtained results are,

$$h_{CS} = h_w + h_{rCS} \quad (14)$$

$$\text{where, } h_w = 5.7 + 3.8V_w \quad (15)$$

$$h_{r_{CS}} = \varepsilon_C \sigma(T_C^4 - T_S^4)(T_C - T_S) \quad (16)$$

$$\text{where } T_S = 0.0552(T_A)^{1.5} \quad (17)$$

The coefficient of heat transfer, h_{PC} from absorber to the cover plate is obtained from,

$$h_{PC} = h_{cPC} + h_{rPC} \quad (18)$$

where the convective heat transfer between absorber plate to cover,

$$h_{cPC} = Nu_c \frac{k_a}{d} \quad (19)$$

$$Nu_c = 0.093(Gr_c)^{0.31} \quad (20)$$

$$Gr_c = \frac{g\beta(T_P - T_C)}{\nu} \quad (21)$$

The radiative heat transfer between absorber plate to cover,

$$h_{rPC} = \frac{\sigma(T_P^2 + T_C^2)(T_P + T_C)}{\frac{1}{\varepsilon_P} + \frac{1}{\varepsilon_C} - 1} \quad (22)$$

The average plate-to-jet air heat transfer coefficients (Chaudhury and Garg, 1991) are,

$$h_{Pj} = Nu_{Pj} \frac{k_a}{d} \quad (23)$$

$$\text{where, } N_{Pj} = F_1 F_2 (Re_D)^m (Z_1/D)^{0.091} \quad (24)$$

The jet Reynolds number, $Re_D = \frac{\rho V_j D}{\mu}$ (25)

For, $1 \le Z_1/D \le 5$, $300 \le \mathrm{Re}_D \le 3 \times 10^4$

The parameters m, F_1, F_2 are evaluated for two Reynolds number ranges; $300 \le \mathrm{Re}_D \le 3000$ and $3000 \le \mathrm{Re}_D \le 3 \times 10^4$. In case of non-cross flow ($\dot{m}_2 = 0$) is considered as $F_2 = 1$, which decreases with an increasing cross flow velocity.

The forced convective coefficients for heat transfer from jet plate to air above (h_{cja2}) be as,

$$h_{cja2} = \frac{A_e}{A} Nu_{ja2} \frac{k_a}{D_2} \quad (26)$$

where, $Nu_{ja2} = 0.0293(Re_{ja2})^{0.8}$, $Re_{ja2} = \frac{(\dot{m}_1+\dot{m}_2)LD_2}{Z_2\mu}$ and

$A_e = A - N\pi D^2 + 2N_1/N$

The radiative heat transfer coefficient between the absorber and jet plate be as,

$$h_{rPj} = \frac{\sigma(T_P^2+T_j^2)(T_P+T_j)}{\frac{1}{\varepsilon_p}+\frac{1}{\varepsilon_j}-1} \quad (27)$$

Similarly, the radiative heat transfer coefficient between jet plate and back plate is,

$$h_{rjb} = \frac{\sigma(T_j^2+T_b^2)(T_j+T_b)}{\frac{1}{\varepsilon_j}+\frac{1}{\varepsilon_b}-1} \quad (28)$$

The bottom loss heat coefficient is calculated by using,

$$U_b = \frac{k_i}{l} \quad (29)$$

The friction factor for a rectangular smooth duct is given as, modified Blasius equation as,

$$f_S = 0.085(Re_{ja2})^{-0.25} \quad (30)$$

The jet air velocity can be calculated from,

$$V_j = \frac{4\dot{m}_1}{\rho N\pi D^2} \quad (31)$$

In the present study, the iteration process has been used for finding the numerical values of the natural convective and radiative heat transfer coefficient for each operational and geometrical parameter, whereas the measured values 1.3 m/s, 30°C and 650 W/m^2 of wind velocity (V_w), ambient temperature (T_A) and solar intensity (I_T) are taken for finding the values of T_o, η_c, h_w, Nu_{Pj}, Re_{ja2} and f_s.

3. RESULTS AND DISCUSSION

3.1 Variation of outlet air temperature and collector efficiency with mass flow rates of air and jet hole diameter

Figs. 7(a-c) and 8(a-c) show the effect of mass flow rates of air ($\dot{m}_1$ and $\dot{m}_2$) and jet hole diameter, D on the outlet air temperature (T_o) and collector efficiency (η_c) respectively in a jet plate solar air heater with longitudinal fins attached underside the absorber surface for fixed pitch of the jet holes, X (60 mm) and depth of the upper channel, Z_2 (80 mm). For all range of the jet hole diameter, D (6 mm-10 mm) under cross flow and non-cross flow conditions of air, it has been observed that the outlet air temperature (T_o) decreases with increase mass flow rates of air ($\dot{m}_1$ and $\dot{m}_2$), whereas collector efficiency (η_c) increases with increase in mass flow air rates of air ($\dot{m}_1$ and $\dot{m}_2$).

Fig. 7 (a-c) shows that the outlet temperature is found higher in case of non-cross flow than cross flow condition of air for fixed mass flow rates of air ($\dot{m}_1$ and $\dot{m}_2$) and jet hole diameter, D. This higher value of outlet air temperature in case of non-cross flow is due to the higher value of cross flow degradation factor ($F_2 = 1$) which is expressed in eqn. (23) for h_{Pj}. The value of F_2 varies from 0 to 1. It becomes maximum 1 for non-cross flow condition and starts decreasing with increase of cross flow of air through the channel.

However, Fig. 8 (a-c) shows that the collector efficiency (η_c) is higher in case of cross flow condition with respect to non-cross flow condition for fixed mass flow rates of air ($\dot{m}_1$ and $\dot{m}_2$) and jet hole diameter, D. Under cross flow and non-cross flow condition of air, the curves clearly indicate the outlet air temperature (T_o) is higher in staggered hole jet plate as compared to inline hole jet plate solar air heater with longitudinal fins, whereas the collector efficiency is found higher in cross flow inline and staggered hole jet plate with respect to non-cross flow inline and staggered hole jet plate solar air heater with longitudinal fins for fixed mass flow rates of air ($\dot{m}_1$ and $\dot{m}_2$) and jet hole diameter, D due to mixing of two flows of air in the upper channel of the air heater. For fixed mass flow rate of air $\dot{m}_1$ (50 kg/hm^2) and jet hole diameter D (6 mm), the increment of outlet air temperature (T_o) is found as 1.9%, 10.2% and 16.97% in non-cross flow staggered hole as compared to cross flow staggered hole, non-cross flow staggered and non-cross flow inline hole jet plate solar air heater with longitudinal fins respectively, whereas the increment of collector efficiency (η_c) is obtained 6.52%, 11.23%, 15.87% in cross flow staggered hole with respect to cross flow inline hole, non-cross flow staggered hole and non-cross flow inline hole jet plate solar air heater with longitudinal fins. The results show the outlet air temperature (T_o) and collector efficiency (η_c) are found higher at lower jet hole diameter, D (6 mm) than higher jet hole diameter, D (8mm and 10 mm) for fixed mass flow rates of air ($\dot{m}_1$ and $\dot{m}_2$) under both cross flow and non-cross flow conditions. These higher values of outlet air temperature (T_o) and collector efficiency (η_c) is due to high jet air velocity (V_j) strikes the lower surface of absorber surface which results to higher outlet air temperature (T_o) and collector efficiency (η_c).

3.2 Effect of jet hole diameter (D) on the collector efficiency (η_c) and absorber plate to jet air heat transfer coefficient (h_{Pj})

The effect of jet hole diameter on the collector efficiency (η_c) and the absorber plate-to-jet air heat transfer coefficient (h_{Pj}) are presented in Figs. 9 (a-c) and 10 (a-c) respectively for fixed pitch of the holes, X (60 mm) and depth of upper channel, Z_2 (8 cm). Under both cross flow and non-cross flow cases, h_{Pj} and η_c increases with decrease in jet hole diameter, D. The examination of the curves reveals that both h_{Pj} and η are increased with decreasing the size of the jet hole in jet plate for fixed mass flow rate ($\dot{m}_1$) and the highest value of h_{Pj} and η_c are found at lowest jet plate hole diameter, because of getting higher jet velocity of air, V_j. This result is similar to the results found by Chaudhury and Garg (1991). For all range of mass flow rates of air ($\dot{m}_1$ and $\dot{m}_2$) and jet hole diameter, D (6mm-10mm), the collector efficiency (η_c) is found higher in case of cross flow staggered hole jet plate, whereas the heat transfer coefficient (h_{Pj}) is observed higher in case of non-cross flow staggered hole jet plate solar air heater with longitudinal fins due to higher value of outlet air temperature (T_o). At fixed value of mass flow rate of air, $\dot{m}_1$ = 50.0 kg/hm^2 and X/D = 10, the increment of collector efficiency (η_c) are found as 4.92%, 9.49% and 13.98% higher in cross flow staggered hole jet plate as compared to cross flow inline hole jet plate, non-cross flow staggered hole and non-cross flow inline hole jet plate solar air heater with longitudinal fins respectively. Similarly, the heat transfer coefficient (h_{Pj}) in non-cross flow inline hole jet plate solar air heater is found as 11.6%, 12.28% and 32.19% higher than cross flow inline and staggered hole jet plate and non-cross flow inline hole jet plate solar air heater with longitudinal fins under same geometrical and operational parameters. It is also observed that the collector efficiency (η_c) and heat transfer coefficient (h_{Pj}) increase with increase in mass flow rates of air ($\dot{m}_1$ and $\dot{m}_2$) in inline or staggered hole jet plate air heater with longitudinal fins for fixed jet hole diameter, D for both the flow conditions of air through the channel.

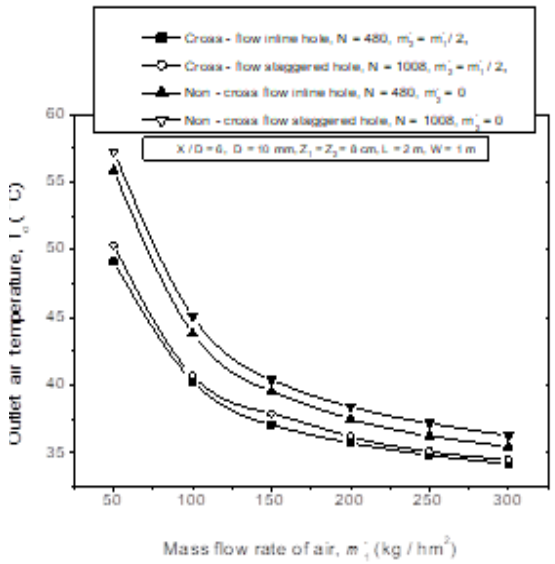

Fig. 7(a) For X/D = 6.0, D = 10 mm, $Z_1 = Z_2$ = 8 cm, L = 2 m, W = 1 m

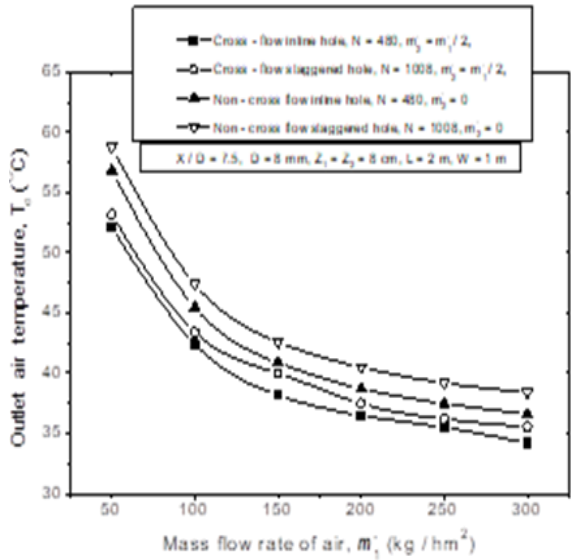

Fig. 7(b) For X/D = 7.5, D = 8 mm, $Z_1 = Z_2$ = 8 cm, L = 2 m, W = 1 m

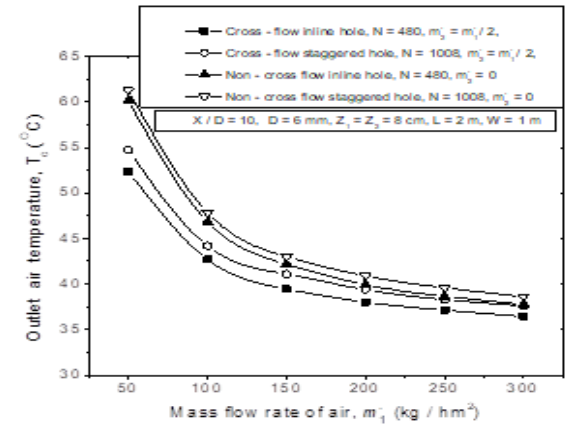

Fig. 7(c) For X/D = 10.0, D = 6 mm, $Z_1 = Z_2$ = 8 cm, L = 2 m, W = 1 m

Fig. 7 Variation of outlet air temperature with mass flow rate of air in cross flow and non-cross flow jet plate solar air heater with longitudinal fins

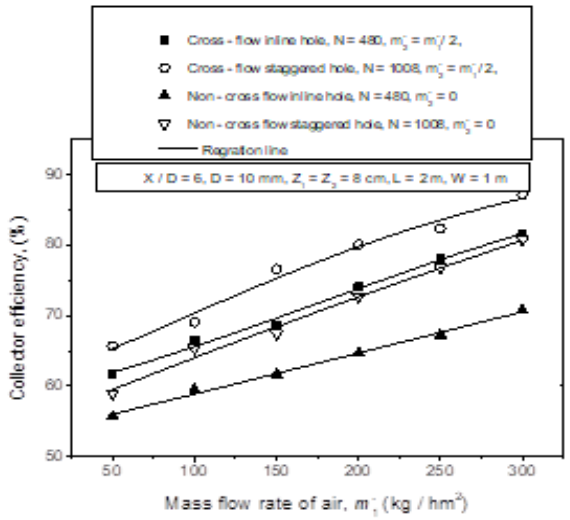

Fig. 8(a) For X/D = 6.0, D = 10 mm, $Z_1 = Z_2$ = 8 cm, L = 2 m, W = 1 m

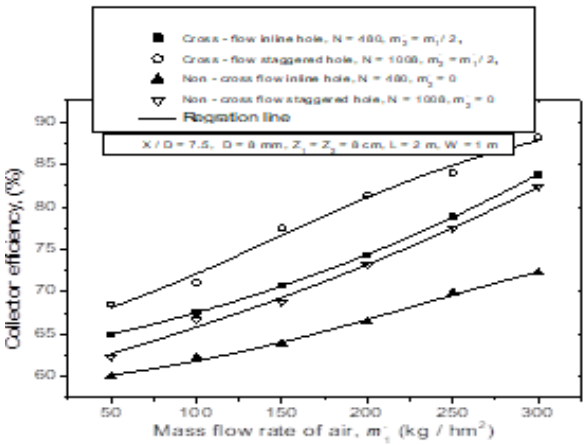

Fig. 8(b) For X/D = 7.5, D = 8 mm, $Z_1 = Z_2$ = 8 cm, L = 2 m, W = 1 m

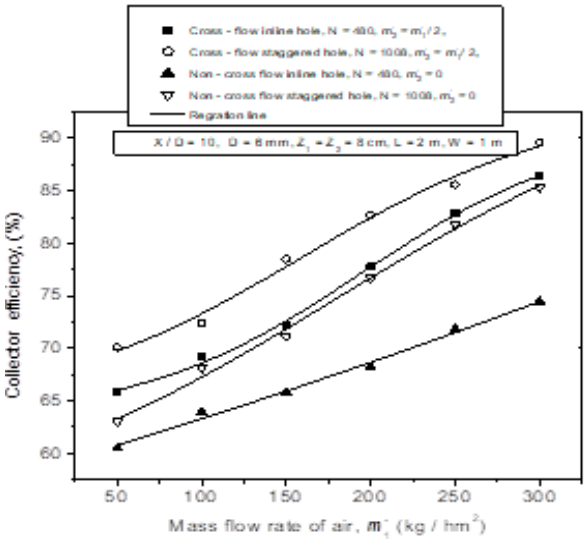

Fig. 8(c) For X/D = 10.0, D = 6 mm, $Z_1 = Z_2$ = 8 cm, L = 2 m, W = 1 m

Fig. 8 Variation of collector efficiency with mass flow rate of air in cross flow and non-cross flow jet plate solar air heater with longitudinal fins

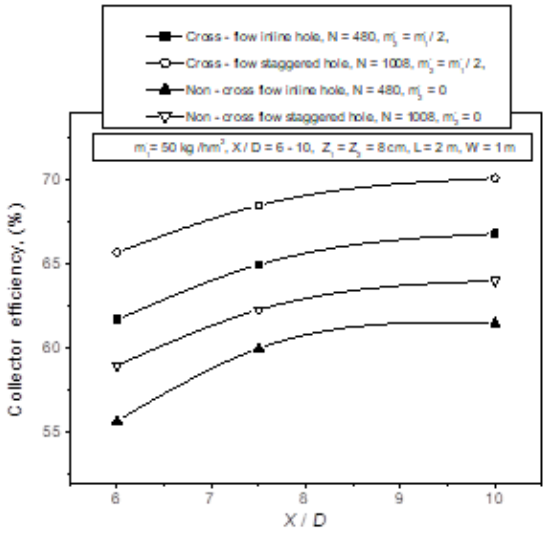

Fig. 9(a) m_1 = 50 kg/hm^3, X/D = 6-10, $Z_1 = Z_2$ = 8 cm, L = 2 m, W = 1 m

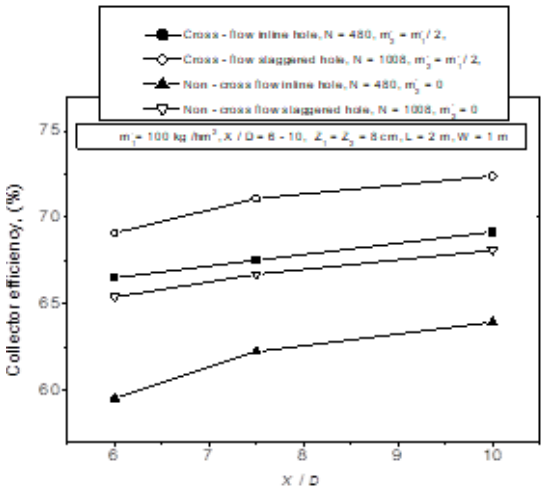

Fig. 9(b) m_1 = 100 kg/hm^3, X/D = 6-10, $Z_1 = Z_2$ = 8 cm, L = 2 m, W = 1 m

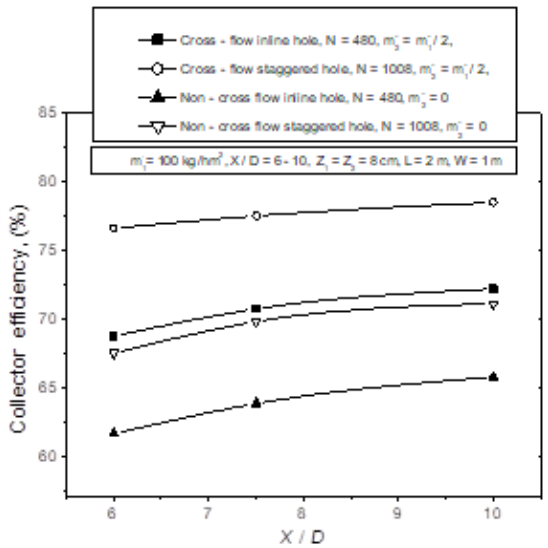

Fig. 9(c) m_1 = 150 kg/hm^3, X/D = 6-10, $Z_1 = Z_2$ = 8 cm, L = 2 m, W = 1 m

Fig. 9 Variation of collector efficiency (η_c) with jet hole diameter (D) for fixed pitch of the jet holes, X (60 mm)

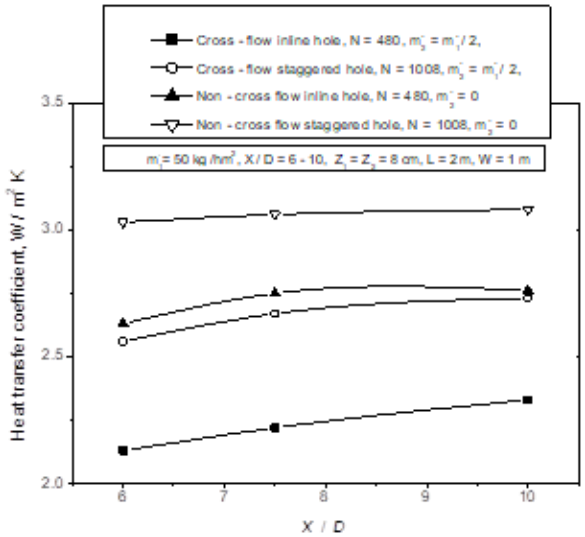

Fig. 10(a) m_1 = 50 kg/hm^3, X/D = 6-10, $Z_1 = Z_2$ = 8 cm, L = 2 m, W = 1 m

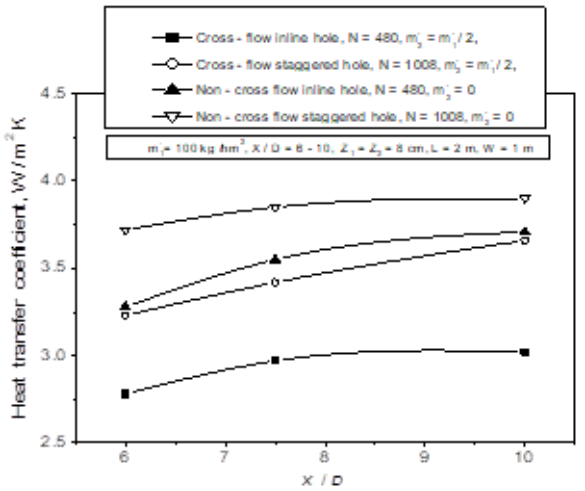

Fig. 10(b) m_1 = 100 kg/hm^3, X/D = 6-10, $Z_1 = Z_2$ = 8 cm, L = 2 m, W = 1 m

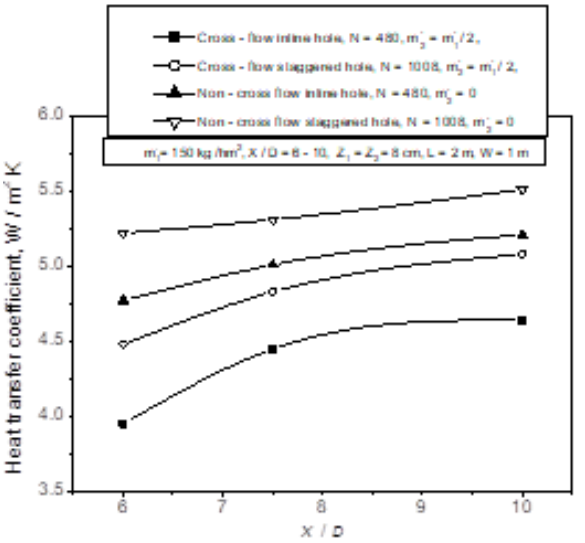

Fig. 10(c) m_1 = 150 kg/hm^3, X/D = 6-10, $Z_1 = Z_2$ = 8 cm, L = 2 m, W = 1 m

Fig. 10 Variation of heat transfer coefficient (h_{pj}) with jet hole diameter (D) for fixed pitch of the jet holes, X (60 mm)

Global Digital Central
ISSN: 2151-8629

3.3 Effect of distance between jet plate and absorber plate (Z_2) on outlet temperature and collector efficiency

The variation of outlet air temperature (T_o) and collector efficiency (η_c) with depth of upper channel (Z_2) for fixed jet hole diameter, D (6 mm) and pitch of holes, X (60 mm) under cross flow and non-cross flow conditions of air are shown in Figs. 11(a) and 11(b) respectively. For fixed mass flow rates of air ($\dot{m}_1$ and $\dot{m}_2$), the results show the outlet air temperature (T_o) and collector efficiency (η_c) decrease with increase in distance between absorber plate and jet plate (Z_2). The higher outlet air temperature (T_o) and collector efficiency (η_c) are found at lower Z_2 (5 cm) with higher mass flow rate of air, $\dot{m}_1$ (100 kg/hm^2) for each air heater. The outlet air temperature (T_o) is found 17.8% higher in non-cross flow staggered hole jet plate solar air heater with respect to cross flow staggered hole jet plate solar air heater with longitudinal fins, whereas the collector efficiency is obtained 2.1% higher in cross flow staggered hole jet plate solar air heater with longitudinal fins for fixed mass flow rate of air, $\dot{m}_1$ (100 kg/hm^2) and depth of upper channel, Z_2 (5 cm).

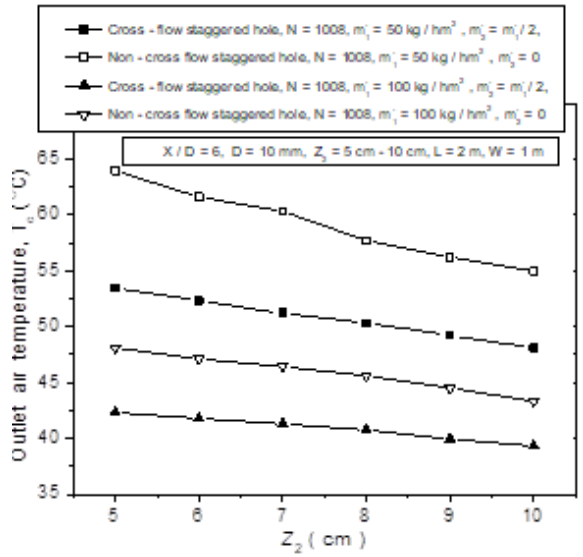

Fig. 11(a) For X/D = 6, D = 10 mm, Z_2 = 5 cm-10 cm, L = 2 m, W = 1 m

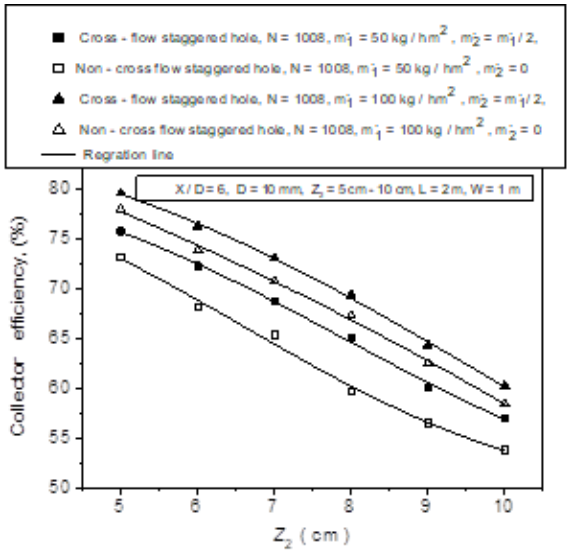

Fig. 11(b) For X/D = 6, D = 10 mm, Z_2 = 5 cm-10 cm, L = 2 m, W = 1 m

Fig. 11 Variation of outlet air temperature (T_o) and collector efficiency (η_c) with depth of upper channel, Z_2 for fixed jet hole diameter, D (10 mm)

3.4 Effect of distance between jet plate and absorber plate (Z_2) on heat transfer coefficient between absorber plate and jet plate (h_{Pj})

Figs. 12(a) and 12(b) show the heat transfer coefficient *(h_{Pj})* and Nusselt number (Nu_{Pj}) respectively, decrease with increase in depth of upper channel (Z_2) for fixed mass flow rates of air ($\dot{m}_1$ and $\dot{m}_2$), jet hole diameter (D) and pitch of the jet holes X (60 mm). However, both the heat transfer coefficient (h_{Pj}) and Nusselt number (Nu_{Pj}) increase with increase in mass flow rates of air for all range of depth of upper channel, Z_2 (5 cm-10 cm). As per the above discussed result, the high outlet air temperature (T_o) results to high heat transfer coefficient (h_{Pj}) and high heat transfer coefficient (h_{Pj}) corresponds to high Nusselt number (Nu_{Pj}) for higher rates of air mass flow through the channel. For all range of mass flow rates of air ($\dot{m}_1$ and $\dot{m}_2$), the results show the heat transfer coefficient (h_{Pj}) and Nusselt number (Nu_{Pj}) are higher in non-cross flow staggered hole as compared to cross flow staggered hole jet plate solar air heater with longitudinal fins. The increment of heat transfer coefficient (h_{Pj}) and Nusselt number (Nu_{Pj}) are found as 12.7% and 15.23% in non-cross flow staggered hole with respect to cross flow staggered hole jet plate solar air heater with longitudinal fins for fixed mass flow rate, $\dot{m}_1$ (100 kg/hm^2).

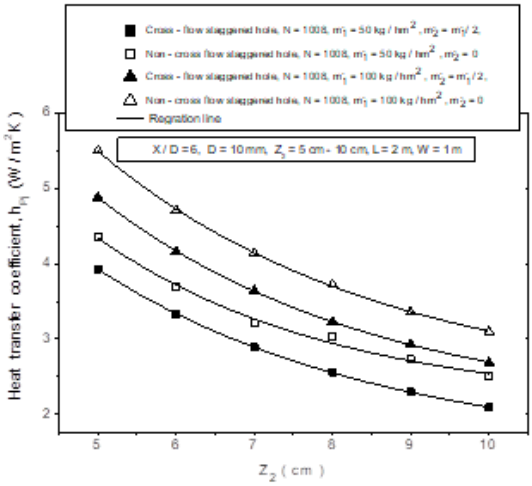

Fig. 12(a) For X/D = 6, D = 10 mm, Z_2 = 5 cm-10 cm, L = 2 m, W = 1 m

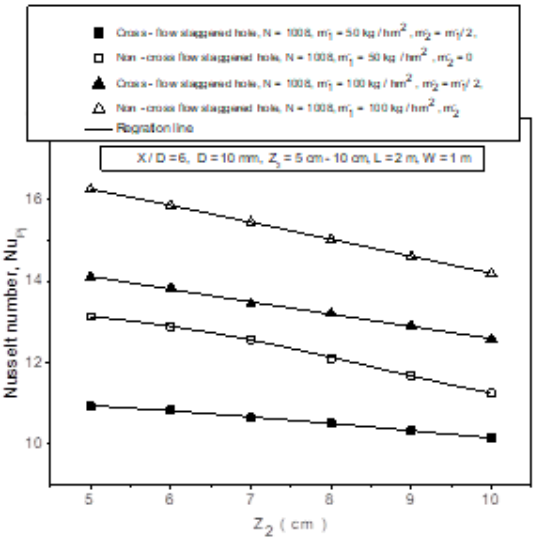

Fig. 12(b) For X/D = 6, D = 10 mm, Z_2 = 5 cm-10 cm, L = 2 m, W = 1 m

Fig. 12 Variation of heat transfer coefficient (h_{pj}) and Nusselt number (Nu_{Pj}) with depth of upper channel (Z_2) for fixed jet hole diameter, D (10 mm)

3.5 Variation of Nusselt number (Nu_{Pj}) with jet hole diameter (D) for fixed depth of upper channel, Z_2 (8 cm) and pitch of the jet holes, X (60 mm)

The effect of jet hole diameter (D) on the Nusselt number (Nu_{Pj}) for fixed depth of upper channel, Z_2 (8 cm) and pitch of the jet holes, X (60 mm) is presented in Fig. 13. The curves show the Nusselt number (Nu_{Pj}) increases with decrease in jet hole diameter (D) for fixed mass flow rate and constant values of X, Z_1 and Z_2. The value of Nusselt number (Nu_{Pj}) in non-cross flow condition is higher as compare to cross flow condition for fixed mass flow rates of air, $\dot{m}_1$ (50 kg/hm^2). For fixed mass flow rates of air ($\dot{m}_1$ and $\dot{m}_2$) and jet hole diameter (D), the present result also complies the above result in which heat transfer coefficient (h_{Pj}) is higher at lower Z_2 due to presence of fluid friction. This higher value of heat transfer coefficient (h_{Pj}) resulting to higher Nusselt number (Nu_{Pj}) in non-cross flow staggered hole jet plate solar air heater with longitudinal fins is observed.

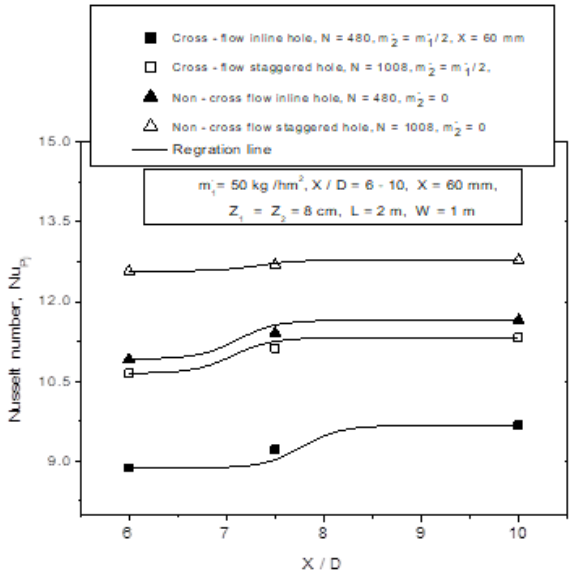

Fig. 13 Variation of Nusselt number (Nu_{Pj}) with jet hole diameter, D (6mm-10mm) for fixed depth of upper channel, Z_2 (8 cm) and pitch of the holes, X (60 mm). For m_1 = 50 kg/hm^3, X/D = 6-10, X = 60 mm, $Z_1 = Z_2$ = 8 cm, L = 2 m, W = 1 m

3.6 Variation of friction factor (f_s) as a function of Reynolds number (Re_{ja2})

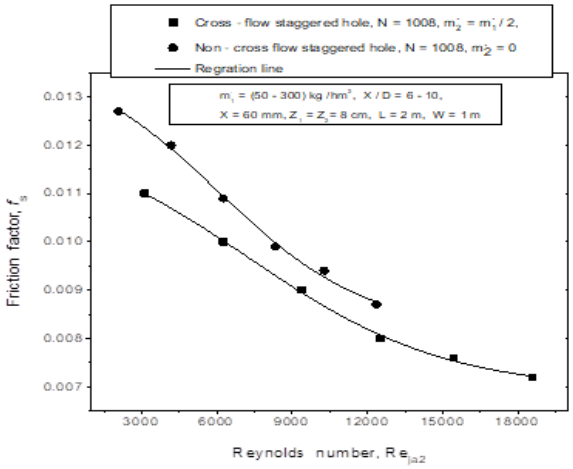

Fig. 14 Variation of friction factor (f_s) with Reynolds number (Re_{ja2}). For m_1 = (50-300) kg/hm^3, X/D = 6-10, X = 60 mm, $Z_1 = Z_2$ = 8 cm, L = 2 m, W = 1 m

Fig. 14 shows the variation of friction factor (f_s) with respect to the Reynolds number (Re_{ja2}) under both cross flow and non-cross flow of air through the channel. It is observed that the friction factor decreases with increase in the Reynolds number (Re_{ja2}) in both cross flow and non-cross flow of air conditions. The curves show the friction factor is higher in case of non-cross flow staggered hole jet plate as compared to cross flow staggered hole jet plate solar air heater with longitudinal fins for all range of Reynolds number (Re_{ja2}). This also complies the above results in which Nusselt number (Nu_{Pj}) is higher at lower jet hole diameter, D (6 mm) and depth of upper channel, Z_2 (5 cm) for given Reynolds number due to presence of fluid friction. This higher value of friction factor results high pressure drop in non-cross flow staggered hole jet plate solar air heater with longitudinal fins. The high pressure drop means the cost of pumping power is more in non-cross flow staggered hole jet plate with respect to cross flow staggered hole jet plate solar air heater with longitudinal fins.

3.6 Variation of fin efficiency (η_f) and fin effectiveness (ξ) of jet plate solar air heater with mass flow rate of air ($\dot{m}_1$) for fixed pitch of the fins (p)

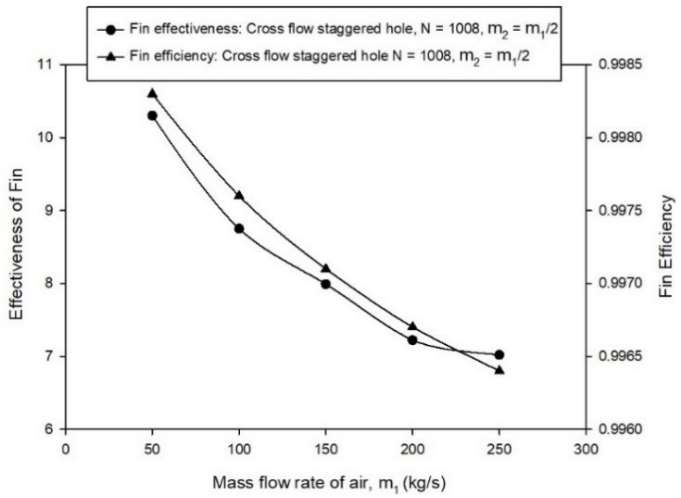

Fig. 15 Variation of efficiency and effectiveness of fin with mass flow rates of air in longitudinal fin staggered hole jet plate solar air heater at fixed jet hole diameter, D (6 mm)

Fig. 15 shows that the variations of the fin efficiency (η_f) and effectiveness of the fin (ξ) with mass flow rates of air $\dot{m}_1$ and $\dot{m}_2$ in longitudinal fin jet plate solar air heater. It is observed that the fin efficiency (η_f) and effectiveness of the fin (ξ) decrease with increase in mass flow rates of air $\dot{m}_1$ and $\dot{m}_2$ for fixed jet hole diameter, D (6 mm). For all range of the fin efficiency (η_f), the value of effectiveness of the fin (ξ) has been found greater than 1 (i.e., $\xi > 1$) indicating the importance of attaching the fins with the absorber plate.

4. CONCLUSIONS

The present analytical work is based on the performance of jet plate solar air heater with longitudinal fins attached underside the absorber surface under cross flow and non-cross flow of air through the channel. From the present study, the following conclusions are made.

1. The outlet air temperature (T_o) and collector efficiency (η_c) are found higher at lower jet hole diameter, D (6 mm) than larger jet hole diameter D (8mm and 10mm) in each air heater for fixed mass mass flow rate of air ($\dot{m}_1$) and depth of upper channel Z_2 (8 cm).
2. For fixed mass flow rate of air ($\dot{m}_1$) and jet hole diameter (D), the outlet air temperature (T_o), heat transfer coefficient (h_{Pj}) and Nusselt number (Nu_{Pj}) are found higher in non-cross flow staggered hole jet plate solar air heater with longitudinal fins than other air heaters.

3. For fixed mass flow rates of air ($\dot{m}_1$ and $\dot{m}_2$), the outlet air temperature (T_o) and collector efficiency (η_c) decrease with increase in depth of upper channel (Z_2).
4. For fixed mass flow rate of air, $\dot{m}_1$ (50-300 kg/hm^2), the outlet air temperature (T_o) and collector efficiency (η_c) are obtained higher at lower Z_2 (5 cm) with respect to larger Z_2 (6 cm-10 cm).
5. For $\dot{m}_1$ (50-300 kg/hm^2), X/D (6.0-10) and Z_2 (8.0 cm), the friction factor (f_s) is obtained higher in case of non-cross flow staggered hole than cross flow staggered hole condition.
6. For all range of Reynolds number (Re_{ja2}), the friction factor (f_s) is higher in case of non-cross flow staggered hole jet plate as compared to cross flow staggered hole jet plate solar air heater with longitudinal fins. The cost of pumping power of the proposed non-cross flow staggered hole jet plate with longitudinal fins air heater is more as compared to cross flow staggered hole jet plate solar air heater with longitudinal fins.

NOMENCLATURE

A	surface area of absorber plate, m^2
A_b	base area of the fin, m^2
A_c	cross-sectional area of the fin, m^2
A_j	area of jet hole, m^2
A_2	cross-sectional area of upper channel, m^2
C_p	specific heat capacity of air, kJ/kg^{o}K
d	air thicness between absorber and cover plate, m
D_2	hydraulic diameter of upper channel in cross flow air heater, m $D_2 = 4\,W\,Z_2 / 2\,(W + Z_2)$
D	diameter of jet hole, m
D_e	equivalent hydraulic diameter of upper channel in jet plate with longitudinal fins solar air heater, m $D_e = 4[pZ_2 - L_f\,\delta_f] / 2[(p + L_f]$
F_1	dimensionless constant
F_2	cross flow degradation factor
f_s	friction factor
h_{Pj}	average plate-to-jet air heat transfer coefficient, W/m^{2}K
I_T	incident solar flux, W/m^2
k_a	thermal conductivity of air flowing through duct, W/mK
k_{Al}	thermal conductivity of the fin material, W/mK
k_i	thermal conductivity of the insulation material
l_i	insulation thickness, m
L	collector length or width of fins, m
L_c	corrected length of the fin, m
L_f	length of the fins, m
m	dimensionless number
m'	Fin parameter, m^{-1}
$\dot{m}_1$	mass flow rate of air through lower channel, kg/sec
N	total number of holes in the jet plate
N_f	total number of fins undersibe the absorber plate
Nu_{Pj}	Nusselt number at upper channel
P_f	perimeter of the fin, m
p	pitch of the fins, m
Q_f	actual rate of heat transfer with fin, W
Q_{mf}	maximum rate of heat transfer from the fin, W
Q_{Nf}	rate of heat transfer without fin, W
Re_{ja2}	flow Reynolds number between absorber plate and jet plate
Re_D	jet Reynolds number
T_A	ambient temperature, ^{o}C
T_{a1}	air temperatur at lower channel, ^{o}C
T_{a2}	air temperatur at upper channel, ^{o}C
T_i	inlet air temperature above jet plate in mixing of air, ^{o}C
T_o	outlet air temperature, ^{o}C
T_{ol}	outlet air temperature at jet hole, ^{o}C
T_P	absorber plate temperature, ^{o}C
$\overline{V}_1$	wetted mean inlet air velocity in the lower channel, m/sec
$\overline{V}_2$	wetted mean inlet air velocity in the upper channel, m/sec
$\overline{V}_o$	wetted mean outlet air velocity in the upper channel, m/sec
V_j	jet air velocity, m/sec
$\overline{V}_{av}$	average velocity of air in the upper channel, m/sec
$\overline{V}$	average velocity of V_{av} and V_o in upper channel, m/sec
X	span-wise pitch of the jet holes, m
Y	stream-wise pitch of jet holes, m
W	width of solar air heater, m
Z_1	distance between the jet plate and bottom plate, m
Z_2	distace between the absorber plate and jet plate, m
ρ	density of air, kg/m^3
δ_f	thickness of the fins, m
μ	dynamic viscosity of air, Pa.sec

Greek Symbols

η	collector efficiency
θ	tilt angle
ξ	effectiveness of the fin
η_f	fin efficiency

Subscripts

Al	aluminum
i	inlet air at upper channel
j	jet air / jet plate
o	*outlet air at heater exit*
ol	outlet air at jet hole
P	absorber plate
t	thickness

REFERENCES

Aboghrara, A.M., Baharudin, B.T.H.T., Alghoul, M.A., Adam, N.M., Hairuddin, A.A., and Hasan, H.A., 2017, "Performance analysis of solar air heater with jet impingement on corrugated absorber plate," *Case Studies in Thermal Engineering*, **10**, 111-120.
https://dx.doi.org/10.1016/j.csite.2017.04.002

Aboghrara, A.M., Alghoul, M.A., Baharudin, B.T.H.T., Elbreki, A.M., Ammar, A.A., Sopian, K., and Hairuddin, A.A., 2018, "Parametric study on the thermal performance and optimal design elements of solar air heater enhanced with jet impingement on a corrugated absorber plate," *International Journal of Photoenergy*, **2018**, 1-22.
https://dx.doi.org/10.1155/2018/1469385

Aharwal, K.R., Gandhi, B.K., and Saini, J.S., 2009, "Heat transfer and friction characteristics of solar air heater ducts having integral inclined discrete ribs on absorber plate," *International Journal of Heat and Mass Transfer*, **52**, 5970-5977.
https://dx.doi.org/10.1016/j.ijheatmasstransfer.2009.05.032

Akpinar, E.K., and Kocyigit, F. 2010, "Experimental investigation of thermal performance of solar air heater having different obstacles on absorber plates," *International Communications in Heat and Mass Transfer*, **37**(4), 416-421.
https://dx.doi.org/10.1016/j.icheatmasstransfer.2009.11.007

Belusko, M., Saman, W., and Bruno, F., 2008 "Performance of jet impingement in unglazed air collector," *Solar Energy,* **82**(5), 389-398.
https://dx.doi.org/10.1016/j.solener.2007.10.005

Chabane, F., Moummi, N., Benramache, S., Bensahal, D., and Belahssen, O., 2013a, "Collector efficiency by single pass of solar air heaters with and without using fins," *Engineering Journal*, **17**(3), 43-55.
https://dx.doi.org/10.4186/ej.2013.17.3.43

Chabane, F., Moummi, N., Brima, A., and Benramache, S., 2013b, "Thermal efficiency analysis of a single-flow solar air heater with different mass flow rates in a smooth plate," *Frontiers in Heat and Mass Transfer*, **4**, 013006, 1-6.
https://dx.doi.org/10.5098/hmt.v4.1.3006

Chabane, F., Moummi, N., and Benramache, S., 2014, "Experimental study of heat transfer and thermal performance with longitudinal fins of solar air heater," *Journal of Advanced Research*, **5**(2), 183-192. https://dx.doi.org/10.1016/j.jare.2013.03.001

Chaudhury, C., and Garg, H.P., 1991, "Evaluation of a jet plate solar air heater," *Solar Energy*, **46**(4), 199-209. https://dx.doi.org/10.1016/0038-092X(91)90064-4

Chauhan, R., and Thakur, N.S., 2013, "Heat transfer and friction factor correlation for impinging jet solar air heater," *Experimental Thermal and Fluid Science,* **44**, 760-767. https://dx.doi.org/10.1016/j.expthermflusci.2012.09.019

Das, S., Biswas, A., and Das, B., 2022, "Numerical analysis of a solar air heater with jet impingement—comparison of performance between jet designs," *Journal of Solar Energy*, **144**(1), 011001. https://dx.doi.org/10.1115/1.4051478

Farahani, S.D., and Shadi, M., 2021, Optimization-decision making of roughened solar air heaters with impingement jets based on 3E analysis, *International Communications in Heat and Mass Transfer*, **129**, 105742. https://dx.doi.org/10.1016/j.icheatmasstransfer.2021.105742

Flilihi, E., Sebbar, E.H., Achemlal, D., Rhafiki, T.E., Sriti, M., and Chaabelasri, E., 2022, "Effect of absorber design on convective heat transfer in a flat plate solar collector: A CFD modeling," *Frontiers in Heat and Mass Transfer*, **18**, 39, 1-6. https://dx.doi.org/10.5098/hmt.18.39

Florschuetz, L.W., Metzger, D.E., and Truman, C.R., 1981, "Jet array impingement with cross flow-correlation of streamwise resolved flow and heat transfer distributions," *NASA Contractor Report*, **3373**. https://ntrs.nasa.gov/api/citations/19810006721/downloads/19810006721.pdf
(Last accessed on 26th January, 2022).

Garg, H.P., Datta, G., and Bandyopadhyay, B., 1983, "A study on the effect of enhanced heat transfer area in solar air heaters," *Energy Conversion and Management*, **23**(1), 43-49. https://dx.doi.org/10.1016/0196-8904(83)90007-9

Garg, H.P., Datta, G., and Bhargava, A.K., 1989, "Performance studies on a finned-air heater," *Energy*, **14**(2), 87-92. https://dx.doi.org/10.1016/0360-5442(89)90082-0

Garg, H.P., Jha, R., Choudhury, C., and Datta, G., 1990, "Theoretical analysis on a new finned type solar air heater," In: Horigome, T., Kimura, K., Takakura, T., Nishino, T., and Fujii, I. (Editors), *International Solar Energy Society Proceedings Series*, Clean and Safe Energy Forever, Pergamon, 537-541. https://dx.doi.org/10.1016/B978-0-08-037193-1.50110-5

Garg, H.P., Jha, R., Choudhury, C., and Datta, G., 1991, "Theoretical analysis on a new finned type solar air heater," *Energy*, **16**(10), 1231-1238. https://dx.doi.org/10.1016/0360-5442(91)90152-C

Gupta, C.L., and Garg, H.P., 1967, "Performance studies on solar air heaters," *Solar Energy*, **11**(1), 25-31. https://dx.doi.org/10.1016/0038-092X(67)90014-X

Gupta, D., Solanki, S.C., and Saini, J.S., 1993, "Heat and fluid flow in rectangular solar air heater ducts having transverse rib roughness on absorber plates," *Solar Energy*, **51**(1), 31-37. https://dx.doi.org/10.1016/0038-092X(93)90039-Q

Hasan, H.A., Sopian, K., Jaaz, A.H., and Al-Shamani, A.N., 2017, Experimental investigation of jet array nanofluids impingement in photovoltaic/thermal collector, *Solar Energy*, **144**, 321-334. https://dx.doi.org/10.1016/j.solener.2017.01.036

Hassan, H., and AboElfadl, S., 2021, "Heat transfer and performance analysis of SAH having new transverse finned absorber of lateral gaps and central holes," *Solar Energy*, **227**, 236-258. https://dx.doi.org/10.1016/j.solener.2021.08.061

Irfan, K., and Emre, T., 2006, "Experimental Investigation of solar air heater with free and fixed fins: Efficiency and exergy loss," *International Journal of Science and Technology*, **1**(1), 75-82. https://citeseerx.ist.psu.edu/viewdoc/download?doi=10.1.1.545.8801&rep=rep1&type=pdf
(Last accessed on 26th January, 2022).

Jourker, A.R., Saini, J.S., and Gandhi, B.K., 2006, "Heat transfer and friction characteristics of solar air heater duct using rib-grooved artificial roughness," *Solar Energy*, **80**(8), 895-907. https://dx.doi.org/10.1016/j.solener.2005.08.006

Karsli, S., 2007, "Performance analysis of new design solar air collectors for drying applications," *Renewable Energy*, **32**(10), 2007, 1645-1660. https://dx.doi.org/10.1016/j.renene.2006.08.005

Kercher, D.M., and Tabakoff, W., 1970, "Heat transfer by a square array of round air jets impinging perpendicular to a flat surface including the effect of spent air," *Journal of Engineering for Gas Turbines and Power,* **92**(1), 73-82. https://dx.doi.org/10.1115/1.3445306

Kumar, N., Kumar, A., and Maithani, R., 2020, Development of new correlations for heat transfer and pressure loss due to internal conical ring obstacles in an impinging jet solar air heater passage, *Thermal Science and Engineering Progress*, **17**, 100493. https://dx.doi.org/10.1016/j.tsep.2020.100493

Kumar, R., Nadda, R., Kumar, S., Kumar, K., Afzal, A., Razak, R.K.A., and Sharifpur, M., 2021a, "Heat transfer and friction factor correlations for an impinging air jets solar thermal collector with arc ribs on an absorber plate," *Sustainable Energy Technologies and Assessments*, **47**, 101523. https://dx.doi.org/10.1016/j.seta.2021.101523

Kumar, S., Thakur, R., Suri, A.R.S., Kashyap, K., Singhy, A., Kumar, S., and Kumar, A., 2021b, "A comprehensive review of performance analysis of with and without fins solar thermal collector," *Frontiers in Heat and Mass Transfer*, **16**(4), 1-11. https://dx.doi.org/10.5098/hmt.16.4

Kurtbas, I., and Turgut, E., 2006, "Experimental investigation of solar air heater with free and fixed fins: Efficiency and energy loss," *International Journal of Science and Technology*, **1**(1), 75-82. https://citeseerx.ist.psu.edu/viewdoc/download?doi=10.1.1.545.8801&rep=rep1&type=pdf
(Last accessed on 26th January, 2022).

Maithani, R., Sharma, S., and Kumar, A., 2021, "Thermo-hydraulic and exergy analysis of inclined impinging jets on absorber plate of solar air heater," *Renewable Energy*, **179**, 84-95. https://dx.doi.org/10.1016/j.renene.2021.07.013

Matheswaran, M.M., Arjunan, T.V., and Somasundaram, D., 2018, "Analytical investigation of solar air heater with jet impingement usingenergy and exergy analysis," *Solar Energy*, **161**, 25-37. https://dx.doi.org/10.1016/j.solener.2017.12.036

McAdams, W.H., 1954, *Heat Transmission*, 3rd ed., McGraw-Hill, New York.

Metzger, D.E., Florschuetz, L.W., Takeuchi, D.I., Behee, R.D., and Berry, R.A., 1979, "Heat transfer characteristics for inline and staggered arrays of circular jets with cross-flow of spent air," *Journal of Heat Transfer*, **101**(3), 526-531. https://dx.doi.org/10.1115/1.3451022

Moshery, R., Chai, T.Y., Sopian, K., Fudholi, A., and Al-Waeli, A.H.A., 2021, "Thermal performance of jet-impingement solar air heater with transverse ribs absorber plate," *Solar Energy*, **214**, 355-366.
https://dx.doi.org/10.1016/j.solener.2020.11.059

Nadda, R., Kumar, Anil, and Maithani, R., 2017, "Developing heat transfer and friction loss in an impingement jets solar air heater with multiple arc protrusion obstacles," *Solar Energy*, **158**, 117-131.
https://dx.doi.org/10.1016/j.solener.2017.09.042

Nayak, R.K., and Singh, S.N, 2016, "Effect of geometrical aspects on the performance of jet plate solar air heater,"*Solar Energy*, **137**, 434-440.
https://dx.doi.org/10.1016/j.solener.2016.08.024

Pazarlioğlu, H.K., Ekiciler, R., and Arslan, K, 2021, "Numerical analysis of effect of impinging jet on cooling of solar air heater with longitudinal fins," *Heat Transfer Research*, **52**(11), 47-61.
https://dx.doi.org/10.1615/HeatTransRes.2021037251

Perry, K.P., 1954, "Heat transfer by convection from a hot gas jet to a plane surface", *Proc. Inst. Mech. Engg.,* **168**(30), 775-780.
https://citeseerx.ist.psu.edu/viewdoc/download?doi=10.1.1.983.110&rep=rep1&type=pdf
(Last accessed on 26th January, 2022).

Prasad, B.N., and Saini, J.S., 1988, "Effect of artificial roughness on heat transfer and friction factor in a solar air heater," *Solar Energy*, **41**(6), 555-560.
https://dx.doi.org/10.1016/0038-092X(88)90058-8

Rajaseenivasan, T., Prasanth, S.R., Antony, M.S., and Srithar, K., 2017, "Experimental investigation on the performance of an impinging jet solar air heater," *Alexandria Engineering Journal*, **56**(1), 63-69.
https://dx.doi.org/10.1016/j.aej.2016.09.004

Romdhane, B.S., 2007, "The air solar collectors: Comparative study, introduction of baffles to favor the heat transfer," *Solar Energy*, **81**(1), 2007, 139-149.
https://dx.doi.org/10.1016/j.solener.2006.05.002

Sahu, M.M., and Bhagoria, J.L., 2005, "Augmentation of heat transfer coefficient by using 90o broken transverse ribs on absorber plate of solar air heater," *Renewable Energy*, **30**(13), 2057-2073.
https://dx.doi.org/10.1016/j.renene.2004.10.016

Salman, M., Chauhan, R., and Kim, S.C., 2021a, Exergy analysis of solar heat collector with air jet impingement on dimple-shape-roughened absorber surface, *Renewable Energy*, **179**, 918-928.
https://dx.doi.org/10.1016/j.renene.2021.07.116

Salman, M., Park, M.H., Chauhan, R., and Kim, S.C., 2021b, Experimental analysis of single loop solar heat collector with jet impingement over indented dimples, *Renewable Energy*, **169**, 618-628.
https://dx.doi.org/10.1016/j.renene.2021.01.043

Salman, M., Chauhan, R., Poongavanam, G.K., Park, M.H., and Kim, S.C., 2022, Utilizing jet impingement on protrusion / dimple heated plate to improve the performance of double pass solar heat collector, *Renewable Energy*, **181**, 653-665.
https://dx.doi.org/10.1016/j.renene.2021.09.082

Shetty, S.P., Madhwesh, N., and Karanth, K.V., 2021, "Numerical analysis of a solar air heater with circular perforated absorber plate," *Solar Energy*, **215**, 416-433.
https://dx.doi.org/10.1016/j.solener.2020.12.053

Singh, S., Chaurasiya, S.K., Negi, B.S., Chander, S., Nemś, M., and Negi, S., 2020, "Utilizing circular jet impingement to enhance thermal performance of solar air heater," *Renewable Energy*, **154**, 1327-1345.
https://dx.doi.org/10.1016/j.renene.2020.03.095

Singh, S.N., 2006, "Performance studies on continuous longitudinal fins solar air heater," *Journal of ISM, Dhanbad*, **2.**

Sivakumar, S., Siva, K., and Mohanraj, M., 2019, Experimental thermodynamic analysis of a forced convection solar air heater using absorber plate with pin-fins, *Journal of Thermal Analysis and Calorimetry*, **136**, 39–47.
https://dx.doi.org/10.1007/s10973-018-07998-5

Soni, A., and Singh, S.N., 2017, "Experimental analysis of geometrical parameters on the performance of an inline jet plate solar air heater," *Solar Energy*, **148**, 149-156.
https://dx.doi.org/10.1016/j.solener.2017.03.081

Sukhatme, S. P., 1996, *Solar energy, Principles of Thermal Collection and Storage*, 2nd ed., Tata McGraw Hill Publishing Company Limited, New Delhi.

Thombre, S.B., and Sukhatme, S.P., 1995, "Turbulent flow heat transfer and friction factor characteristics of shrouded fin arrays with uninterrupted fins," *Experimental Thermal and fluid Science*, **10**(3), 388-396.
https://dx.doi.org/10.1016/0894-1777(94)00059-H

Verma, R., Chandra, R., and Garg, H.P., 1991, "Parametric studies on the corrugated solar air heaters with and without cover," *Renewable Energy*, **1**(3-4), 361-371.
https://dx.doi.org/10.1016/0960-1481(91)90045-Q

Vinod, P.D., and Singh, S.N., 2017, Thermo-hydraulic performance analysis of jet plate solar air heater under cross flow condition, *International Journal of Heat and Technology*, **35**(3), 603-610.
https://dx.doi.org/10.18280/ijht.350317

Xing, Y., Spring, S., and Weigand, B., 2010, "Experimental and numerical investigation of heat transfer characteristics of inline and staggered arrays of impinging jets," *Journal of Heat Transfer*, **132**(9), 092201.
https://dx.doi.org/10.1115/1.4001633

Yadav, S., and Saini, R.P., 2020, "Numerical investigation on the performance of a solar air heater using jet impingement with absorber plate,"*Solar Energy*, **208**, 236-248.
https://dx.doi.org/10.1016/j.solener.2020.07.088

Yadav, S., and Saini, R.P., 2022, Thermo-hydraulic CFD analysis of impinging jet solar air heater with different jet geometries, In: Kumar, R., Pandey, A.K., Sharma, R.K., and Norkey, G. (Editors), *Recent Trends in Thermal Engineering*, Lecture Notes in Mechanical Engineering. Springer, Singapore, 193-201.
https://dx.doi.org/10.1007/978-981-16-3132-0_19